



|              |  |
|--------------|--|
| Title        | Prediction of the Strength of Joints between Dissimilar Elastic Materials(Mechanics, Strength & Structural Design) |
| Author(s)    | Murakawa, Hidekazu; Serizawa, Hisashi; Chiaki, Sadayoshi et al.  |
| Citation     | Transactions of JWRI. 2003, 32(2), p. 343-348  |
| Version Type | VoR  |
| URL          | <a href="https://doi.org/10.18910/6529">https://doi.org/10.18910/6529</a>  |
| rights       |  |
| Note         |  |

*The University of Osaka Institutional Knowledge Archive : OUKA*

<https://ir.library.osaka-u.ac.jp/>

The University of Osaka

# Prediction of the Strength of Joints between Dissimilar Elastic Materials<sup>†</sup>

MURAKAWA Hidekazu\*, SERIZAWA Hisashi\*\*, CHIAKI Sadayoshi\*\*\*  
and ODA Isamu\*\*\*\*

## Abstract

To clarify the influence of various factors on the strength of the joint between dissimilar materials, serial computations are conducted using the interface element. Based on the computed results, a dimensionless parameter is derived from the similarity. Further more the relation between this dimensionless parameter and the mode of failure process are closely examined.

**KEY WORDS:** (Joint Strength) (Dissimilar Materials) (Interface) (Interface Element) (Surface Energy) (Scale Parameter) (Similarity) (Master Curve)

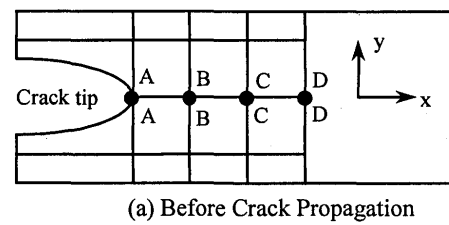
## 1. Introduction

The strength of the joint between dissimilar materials is influenced by the mechanical properties of the interface and the materials to be joined. The geometry of the joint is also influential. To study the influences of various parameters, the level of stress and the order of the singularity in the stress field are commonly employed for the relative evaluation of the strength. Although detailed information on the stress field is obtained, little information on the criteria of the fracture is available from these types of study. This comes from the fact that the physics of failure itself is not explicitly modeled. The cohesive element<sup>1)</sup> or the interface element<sup>2-4)</sup>, which directly models the formation of the surface, may have potential capability not only to give insight into the criteria of the fracture but also to make the quantitative prediction of strength itself. In this report, the influences of the various parameters on the strength of joints between dissimilar elastic materials are investigated using the interface element. Based on the computed results, the similarity holds for the strength of the joint and the processes of failure are closely examined.

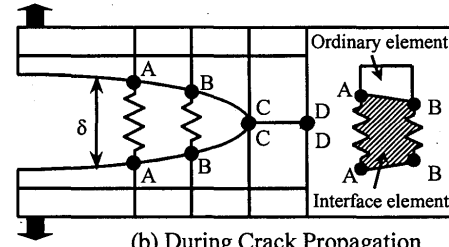
## 2. Interface Element

Essentially, the interface element employed in this research is the distributed nonlinear spring existing

between surfaces forming the interface or the potential crack surfaces as shown by Fig.1. The relation between the opening of the interface  $\delta$  and the bonding stress  $\sigma$  is shown in Fig.2. When the opening  $\delta$  is small, the bonding between the two surfaces is maintained. As the opening  $\delta$  increases, the bonding stress  $\sigma$  increases till it becomes the maximum value  $\sigma_{cr}$ . With further increase of  $\delta$ , the bonding strength is rapidly lost and the surfaces are completely separated. Such interaction between the surfaces can be described by the interface potential. There are rather wide choices for such potentials<sup>1,2)</sup>. The authors employed the Lennard-Jones type potential  $\phi$



(a) Before Crack Propagation



(b) During Crack Propagation

Fig.1 Modeling of crack extension.

† Received on Dec. 1, 2003

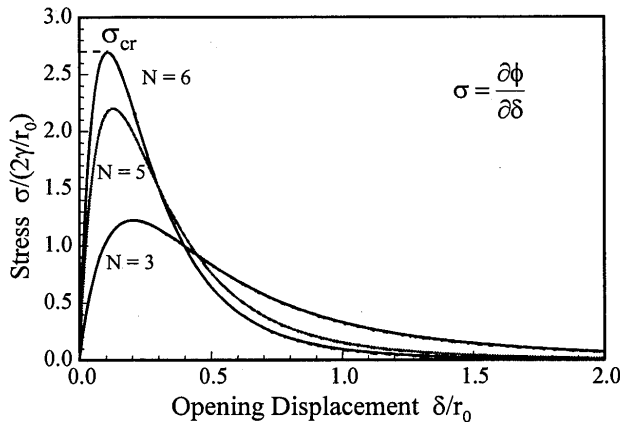
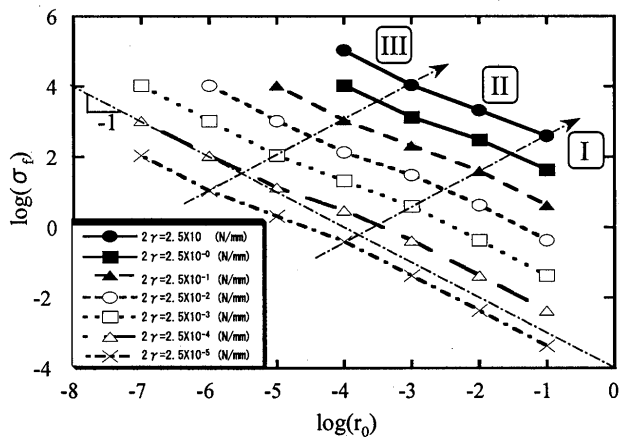
\* Professor

\*\* Associate Professor

\*\*\* National Maritime Research Institute

\*\*\*\* Graduate Student

Transactions of JWRI is published by Joining and Welding Research Institute of Osaka University, Ibaraki, Osaka 567-0047, Japan


 Fig.2  $\sigma$ - $\delta$  relation of interface element.

 Fig.4 Influence of  $\gamma$  and  $r_0$  on joint strength.

because it explicitly involves the surface energy  $\gamma$ , which is necessary to form new surfaces, i.e.

$$\phi(\delta) = 2\gamma \cdot \left\{ \left( \frac{r_0}{r_0 + \delta} \right)^{2N} - 2 \cdot \left( \frac{r_0}{r_0 + \delta} \right)^N \right\} \quad (1)$$

where, constants  $\gamma$ ,  $r_0$ , and  $N$  are the surface energy per unit area, the scale parameter and the shape parameter of the potential function. The derivative of  $\phi$  with respect to the opening displacement  $\delta$  gives the bonding stress  $\sigma$  acting on the interface.

$$\sigma = \frac{\partial \phi}{\partial \delta} = \frac{4\gamma N}{r_0} \cdot \left\{ \left( \frac{r_0}{r_0 + \delta} \right)^{N+1} - \left( \frac{r_0}{r_0 + \delta} \right)^{2N+1} \right\} \quad (2)$$

As is seen from the above equation, the bonding stress  $\sigma$  is proportional to the surface energy  $\gamma$  and inversely proportional to the scale parameter  $r_0$ . By arranging such interface elements along the crack propagation path as shown in Fig.1, the growth of the crack under the applied load can be analyzed in a natural manner. In this case, a decision on the crack growth based on the comparison between the driving force and the resistance as in the conventional methods is not necessary.

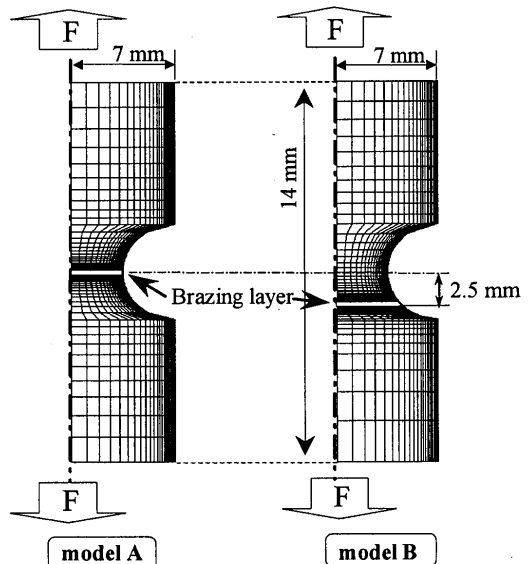


Fig.3 Brazed joint model.

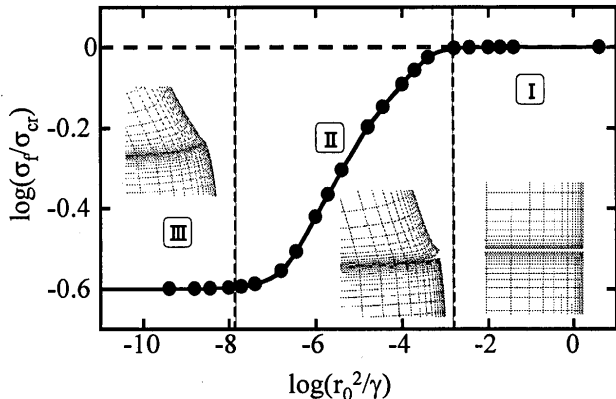
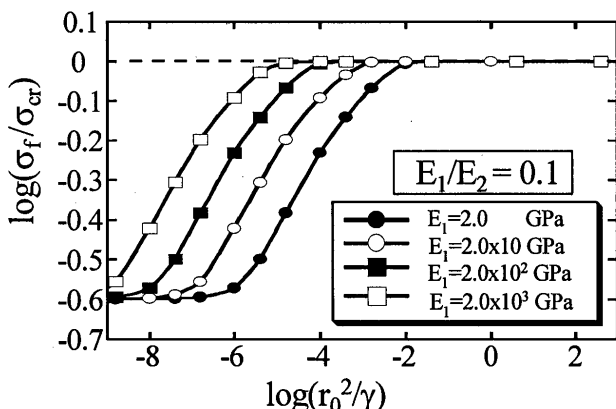
### 3. Brazed Joint Model for Analysis

The model to be analyzed is a brazed stainless steel joint. The mechanical properties of the interface can be characterized by the two parameters, namely the surface energy  $\gamma$  and the scale parameter  $r_0$  when the shape parameter  $N$  is fixed. Thus these parameters can be determined by experiments using specimens with two different joint geometries. Figure 3 shows the two specimens to be analyzed. The Model-A has the brazing layer at the center of the specimen and the Model-B has the brazing layer 2.5 mm away from the center. The thickness of the brazing layer is 40  $\mu$ m. According to the test results, the joint fails after significant plastic deformation. Though this problem must be discussed as an elastic-plastic problem, it is simplified as an elastic problem to extract the fundamental features involved. Since the hardness of the brazing layer is much higher than the base metal, the brazing layer remains in an elastic state and the plastic deformation is fully developed in the base metal.

Considering this, both the base metal and the brazing metal are assumed as elastic materials and the Young's modulus of the base metal is 1/10 of that of the brazing layer. The interface elements are arranged on both sides of the brazing layer. The problem is analyzed as an axisymmetric problem. The maximum load or the load at the loss of static equilibrium is taken as the failure load and the failure strength  $\sigma_f$  is defined as the average stress over the area of the joint.

### 4. Influence of Interface Parameters on Joint Strength

To clarify the influence of the surface energy  $\gamma$  and the scale parameter  $r_0$ , serial computations are made

Fig.5 Influence of  $r_0^2/\gamma$  on failure process.Fig.7 Influence of  $E_1$  on joint strength.

using the Model-A as an example. In the serial computations, the Young's modulus of the base metal  $E_1$ , that of brazing layer  $E_2$  and their Poisson's ratio  $\nu$  are assumed to be 20 GPa, 200 GPa and 0.3. The fracture strength  $\sigma_f$  is computed by changing the surface energy  $2\gamma$  from  $2.5 \times 10^{-5}$  (N/mm) to 25 (N/mm) and the scale parameter  $r_0$  from  $1.0 \times 10^{-1}$  (mm) to  $1.0 \times 10^{-7}$  (mm). As summarized in Fig.4, the joint strength increases with the surface energy  $\gamma$  and decreases with the scale parameter  $r_0$ . It is seen that all curves consist of three zones. In zones I and III, the slopes of the curves are -1 or  $\sigma_f$  is proportional to  $1/r_0$ . While in the zone II, the slope is greater than -1. The reason for this will be discussed in the next section together with the similarity.

## 5. Similarity

Since all the curves in Fig.4 seem to be shifted with keeping their shape, the curves are re-plotted  $\log(\sigma_f/\sigma_{cr})$  as ordinate and  $\log(r_0^2/\gamma)$  as abscissa in Fig.5. All the curves coincide with each other and a single curve is obtained. To closely examine the process of the failure, the deformations at the edge of the interface just before failure are shown for the three zones. It is clearly seen that the base metal and the brazing layer are simply

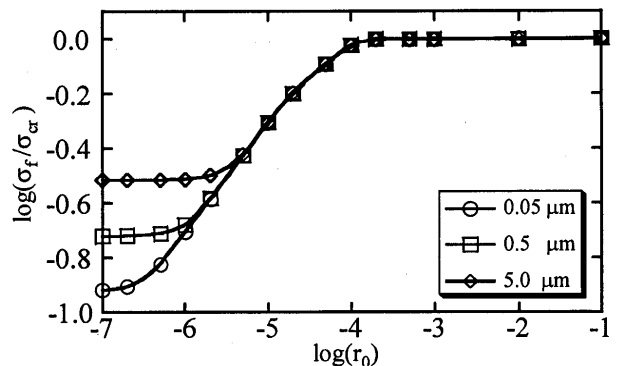


Fig.6 Influence of mesh size on joint strength.

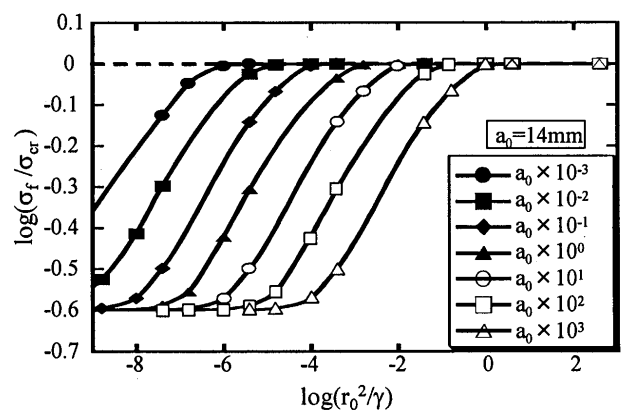


Fig.8 Influence of specimen size on joint strength.

separated without significant deformation in the zone-I. In the zone-II, crack-like localized opening is observed at the edge of the interface. The joint breaks suddenly without significant opening of the interface in the zone-III.

These processes of failure can be related to the joint strength in the following way. Since the opening deformation of the interface is dominant, the strength of the joint is almost the same as the bonding strength  $\sigma_{cr}$  in the zone-I. According to Eq.(2), both the stiffness and the strength of the interface are small in zone-I. Thus, the joint breaks in the simple separation mode. On the other hand when the scale parameter  $r_0$  is small as in the zone-III, bonding strength becomes larger than the stress induced at the crack tip in the FEM model. In this case, the crack-like localized opening is not formed and the failure occurs when the computed stress at the edge of the interface reaches the critical stress  $\sigma_{cr}$ . Since this phenomenon is caused by the coarseness of the mesh, it can be eliminated by using small enough mesh divisions.

To examine the influence of the mesh size, the strength of the joint is computed using different mesh sizes. Three cases in which the sizes of the element at the edge of the interface are 5.0, 0.5 and 0.05  $\mu\text{m}$  are

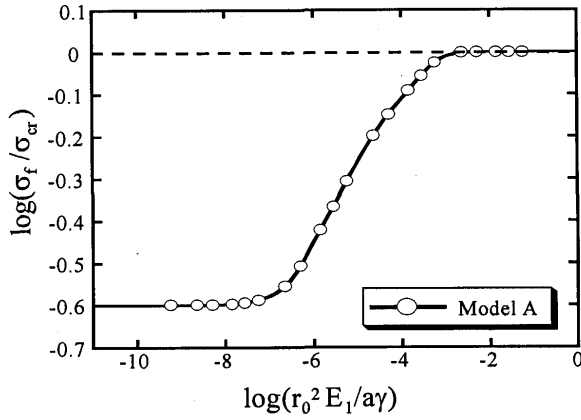
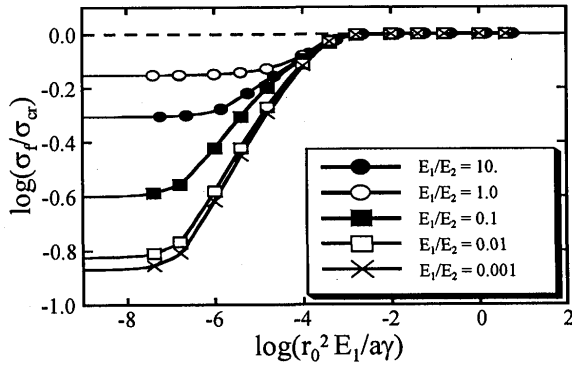
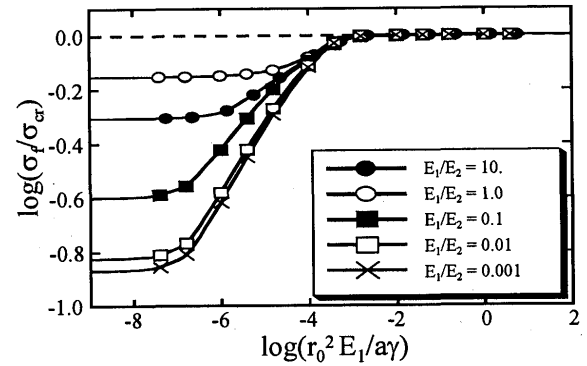

 Fig.9 Master curve in terms of  $r_0^2 E_1/ay$ .


Fig.11 Influence of joint geometry.

compared. As plotted in Fig.6, the joint strength in zone-I and zone-II are mesh insensitive. While, in the zone-III it is mesh dependent because of the reason discussed in the preceding section. When the size of the element is 0.05 mm, the computed curve for the joint strength is reliable if the scale parameter,  $r_0$ , is greater than  $10^{-6}$  mm.

To clarify the influence of the Young's modulus of the material, the strengths of the joints with different values of  $E_1$  ranging from 2.0 GPa to  $2.0 \times 10^3$  GPa are computed, keeping the ratio  $E_1/E_2$  as 0.1. The joint strength increases with the Young's modulus as shown in Fig.7. Similarly the scale effect on the joint strength is examined by changing the size of the specimen from 1/1000 to 1000 times of the standard specimen. As summarized in Fig.8, the joint strength increases when the size becomes smaller.

As seen from the above, the Young's modulus and the scale of the specimen are influential in the joint strength, as well as the properties of the interface. It is also observed that all curves in Figs.7 and 8 have similarity. Thus, all of the computed results are rearranged with respect to a dimensionless parameter  $r_0^2 E_1/ay$ , where  $a$  is the representative dimension of the


 Fig.10 Influence of  $E_1/E_2$  on joint strength.

specimen. All the curves are unified into a single master curve in Fig.9. The physical meaning of the dimensionless parameter is given in the Appendix.

## 6. Influence of Ratio of Young's Moduli and Geometry on Strength of Joint

The influence of the ratio between the Young's modulus of the materials on the strength of the joint is examined by changing the ratio  $E_1/E_2$  in the computation. The master curves for cases with different  $E_1/E_2$  ratios are compared in Fig.10. The joint strength becomes the maximum when  $E_1/E_2=1.0$ . The strength decreases when  $E_1/E_2$  becomes greater or smaller than 1.0. The influence of the joint geometry on the master curve is also examined by comparing Model-A and Model-B shown in Fig.3. As shown in Fig.11, the strength of the Model-B is relatively higher compared to the Model-A, which has the brazing layer at the center.

## 7. Conclusions

Serial computations using the interface element are conducted to clarify the influence of various factors on the strength of the joint between dissimilar materials. Through these computations, the following conclusions are drawn.

- (1) A similarity holds for the strength of the joint between dissimilar elastic materials. Based on this similarity, a master curve for the joint strength can be drawn as a function of a dimensionless parameter  $r_0^2 E_1/ay$ .
- (2) The master curve consists of three zones. Among the three zones, the zone-I and the zone-II have physical meanings and they correspond simple separation and fracture accompanying formation of localized opening.
- (3) The mechanical property of the interface can be characterized by the two parameters, namely the surface energy  $\gamma$  and the scale parameter  $r_0$  when the shape parameter  $N$  is fixed.

## References

- 1) Needleman, A. : An Analysis of Decohesion Along an Imperfect interface, *Int. J. of Fracture*, No.42 (1990), 21-40.
- 2) Murakawa, H., Serizawa, H. and Wu, Z. : Crack Propagation Analysis Using Interface Element (Report I) - Theoretical Formulation and Potential Fields of Application -, *Trans. of JWRI*, Vol. 27 (1998), No.2, 67-72.
- 3) Murakawa, H. and Wu, Z. (1999): "Computer Simulation Method for Crack Growth Using Interface Element Employing Lennard-Jones Type Potential Function, *Materials Science Research International*, Vol. 5 (1999), No. 3, 195-201.
- 4) Murakawa, H., Serizawa, H., Wu, Z. and Shibahara M. : Strength Analysis of Joint between Dissimilar Materials Using Interface Element, *Materials Science Research International, Special Technical Publication-2* (2001), 209-213.

## Appendix A Simple Model to Illustrate Modes of Failure and Similarity

As discussed in the text, the strength of the joint between dissimilar materials can be characterized by a single curve with respect to a dimensionless parameter  $r_0^2 E_1 / a \gamma$  when the ratio between the Young's moduli of the two materials and the shape of the joint are the same. This can be explained using a simple model shown in Fig.A-1. The model consists of linearly connected two elements. One on the top represents an elastic-plastic continuum in the three dimensional space. The other one on the bottom represents a potential failure surface.

The mechanical properties of these two nonlinear springs are characterized by the following sets of parameters,  $(\gamma, r_0)$  and  $(E, \sigma_Y, h)$ , respectively. The parameters  $\gamma$  and  $r_0$  are the surface energy and the scale parameter of the interface. The parameters  $E$ ,  $\sigma_Y$  and  $h$  are the Young's modulus, the yield stress and the strain hardening coefficient. It is readily expected that the spring system shows variety of responses under the applied load  $F$  depending on the combination of these

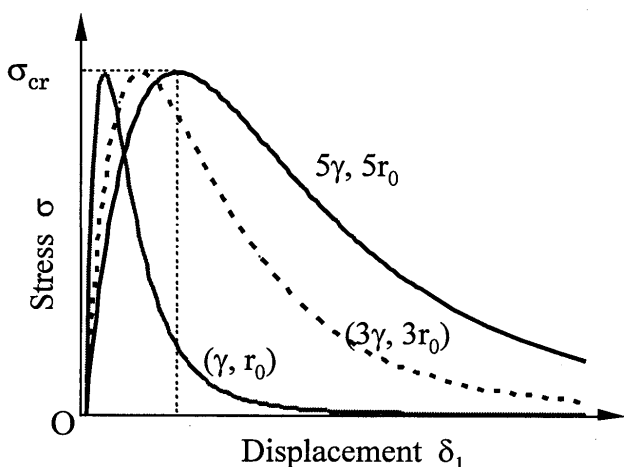


Fig.A-2 Mechanical property of interface.

parameters. In this example, the property of the interface element is changed as shown in Fig.A-2. The three cases in which the surface energy  $\gamma$  and the scale parameter  $r_0$  are changed among  $(\gamma, r_0)$ ,  $(3\gamma, 3r_0)$  and  $(5\gamma, 5r_0)$ , while keeping the critical stress  $\sigma_{cr}$  the same, are considered. The mechanical behavior of the elastic-plastic continuum can be represented by the force-displacement curve shown in Fig.A-3. When  $\sigma_{cr} < \sigma_Y$ , the system remains in an elastic state. The load displacement relations of the system with three different interface elements are shown in Fig.A-4. When both the surface energy and the scale parameter are large, such as in the case of  $(5\gamma, 5r_0)$ , the system remains in the static equilibrium until the complete loss of the strength. On the contrary, the system fails suddenly by losing the stability as in the case of brittle fracture when both of them are small, as in the case of  $(\gamma, r_0)$ .

The same example can be used to obtain the dimensionless parameter, which characterizes the behavior of the system. When the systems are similar, the ratio between the initial stiffness of the two springs must be the same. Assuming that the continuum element has a cubic shape with size  $a$ , the initial stiffnesses  $K_1$  of the spring-1 and  $K_2$  of the spring-2 satisfy the following relations.

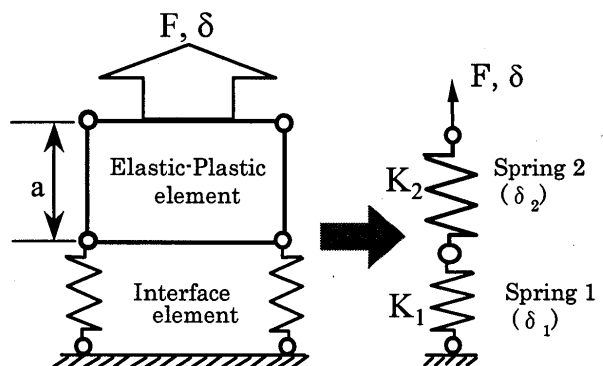


Fig.A-1 Linear spring system.

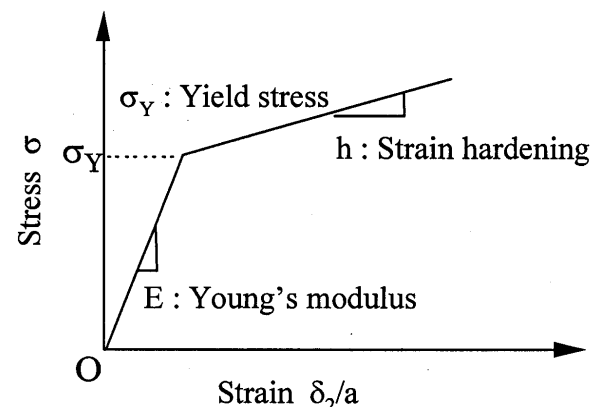


Fig.A-3 Mechanical property of elastic-plastic continuum.

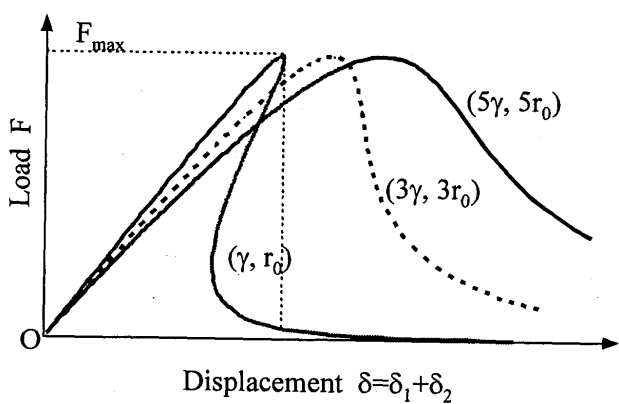


Fig.A-4 Modes of failure of elastic system.

$$K_1 \propto \gamma a^2 / (r_0)^2 \quad (A-1)$$

$$K_2 \propto E a \quad (A-2)$$

By taking the ratio  $K_2/K_1$ , the dimensionless parameter  $r_0^2 E_1 / a\gamma$  is derived. This tells us that the behavior of the system becomes similar when the parameter  $r_0^2 E_1 / a\gamma$  is the same.

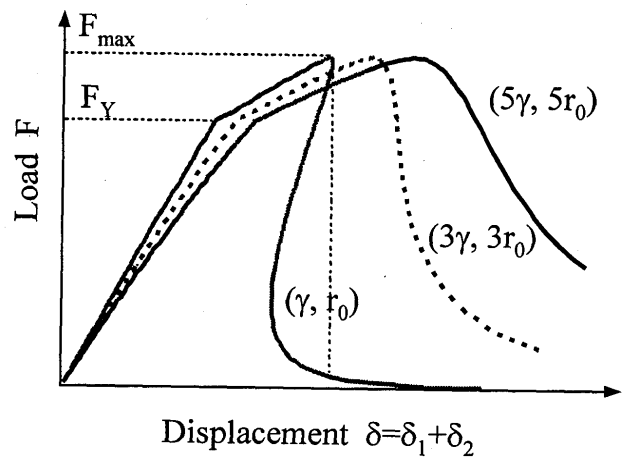


Fig.A-5 Modes of failure of elastic-plastic system.

Similarly, the load-displacement curve when  $F_{max} > F_Y$  is shown in Fig.A-5. In this case, the phenomenon becomes elastic-plastic and the similarity can be expected when the three parameters ( $K_2/K_1 \propto r_0^2 E_1 / a\gamma$ ), ( $F_{cr}/F_Y \propto \gamma \sigma_Y r_0$ ) and ( $h/E$ ) are the same.